



OPEN Altered levels of angiogenin and tRNA-derived fragments associate with severe asthma

Clara Claus^{1,5}, Julieta B. Grosso^{1,5}, María Belen Maraval¹, Matias Arduoso^{2,3}, Oscar A. Bottasso¹, Tania Maes⁴, Ken Bracke⁴, Guy Brusselle⁴, Mauro Ibañez¹, Ledit R. F. Arduoso^{2,3} & Silvana V. Spinelli¹✉

Recent discoveries highlight angiogenin (ANG) and 5' tRNA-derived fragments as key factors in stress response and cell survival. To explore their role in asthma pathogenesis, particularly in severe cases, we evaluated the levels of ANG and 5' tRNA halves (tRHs) derived from tRNA Glu (5'-tRH Glu: tRF-32-87R8WP9N1EWJM) and tRNA Gly (5'-tRH Gly: tRF-30-PNR8YP9LON4V), two abundant tRHs in the respiratory tract, in sputum and blood samples from asthmatic patients. We found ANG expression is significantly increased in circulating leukocytes from severe asthma patients but not in sputum infiltrates. On the contrary, tRHs levels showed significant alterations only in extracellular compartments. Both tRHs were downregulated in the plasma of asthmatic patients, while elevated 5'-tRH Gly levels were observed in severe sputum samples, indicating tissue-specific roles in disease pathology. Additionally, tRH expression in leukocytes was negatively associated with the disrupted corticosteroid response in asthmatic patients. Altered levels of ANG and 5'-tRH Glu and 5'-tRH Gly were further validated in an in vitro model of pollutant-aggravated, allergen-stimulated macrophages. In summary, our findings provide new insights into the role of ANG and tRHs in asthma pathogenesis, highlighting their potential as novel markers for asthma phenotyping.

Keywords Asthma, Angiogenin, tRNA-derived fragments, tRH, Stress

Asthma is one of the most common lifelong inflammatory diseases, affecting around 300 million people worldwide. It is characterized by reversible airway obstruction, airway hyperresponsiveness (AHR), together with inflammation, and structural changes at such level¹.

In the past decades, asthma has been increasingly recognized as a complex disease encompassing different phenotypes and endotypes. The heterogeneity of asthma in terms of onset, natural course and response to treatment is one of the main obstacles to developing efficient strategies to reduce the global asthma burden^{2,3}.

Traditional asthma biomarkers include eosinophils, neutrophils, IgE, periostin, fraction of exhaled nitric oxide (FeNO), and leukotrienes. It has been shown that the use of biomarkers contributes to a better diagnosis, predict exacerbations and prompt treatment. In this regard, exhaled air FeNO and blood eosinophils are easily measurable biomarkers that can be used to monitor patients, although their usefulness in reliably predicting severe cases is controversial^{4–6}.

Anti-inflammatory corticosteroids serve as the cornerstone in the management of asthma and are frequently co-administered with short- or long-acting β_2 -adrenoceptor agonists, commonly known as bronchodilators⁷. These combined therapeutic approaches enable the majority of asthma individuals to effectively control their symptoms. However, a notable subset of the asthma population, comprising 5–10%, exhibits limited benefit of glucocorticoid (GC) therapy⁸. Such GC insensitivity represents a challenge in managing severe asthmatics and highlights the profound alteration in the physiological stress response of these patients.

Recent findings identified new molecular pathways responsible for regulating cell survival under stress conditions that involve the ribonuclease angiogenin (ANG) and tRNA derived fragments^{9,10}.

Although tRNAs are primarily known as adapter molecules crucial for translation, growing experimental evidence suggests that tRNAs are not merely end products but can also serve as sources of functional small

¹Institute of Clinical and Experimental Immunology of Rosario (IDICER CONICET-UNR), Rosario, Argentina. ²Allergy and Immunology Department, Hospital Provincial del Centenario, Rosario, Argentina. ³Clinical Research Center of the Institute of Health Specialties of Rosario (CIC-IESR), Rosario, Argentina. ⁴Department of Respiratory Medicine, Ghent University Hospital, Ghent, Belgium. ⁵Clara Claus and Julieta B. Grosso have contributed equally to this work. ✉email: spinelli@idicer-conicet.gob.ar

RNAs. These molecules have recently been linked to a conserved array of biological processes, including gene regulation in cell metabolism, immune responses, transgenerational inheritance, development, and cancer^{11,12}. Various studies have shown that the accumulation of tRNA fragments is triggered by a variety of stress stimuli, such as oxidative stress, heat shock, and UV radiation, but they are also detected under non-stress conditions^{11,13}. The biogenesis of these fragments involves specific RNA nucleases and is modulated by stress conditions and RNA modifications through mechanisms that remain not entirely defined¹¹.

Angiogenin (ANG) is a protein belonging to the RNase A superfamily. Although initially identified in 1985 for its role in inducing angiogenesis, ANG is now recognized for its involvement in a myriad of physiological and pathological processes¹⁴. Intriguingly, the ribonuclease activity of ANG plays a crucial role in many of these processes, and recent investigations have pinpointed tRNAs as its specific *in vivo* targets⁹.

The cleavage of tRNAs by ANG takes place in the anticodon loop, generating tRNA halves of approximately 30–35 nucleotides. Under conditions of cellular stress, ANG migrates from the nucleus to the cytoplasm, leading to the induction of tRH production and contributing to cell survival. These molecules play biological roles through a variety of mechanisms by interacting with proteins or mRNA, inhibiting translation, and regulating gene expression, the cell cycle, and chromatin and epigenetic modifications^{10,11,15}. Interestingly, recent studies by Dutta and colleagues show that while Angiogenin is responsible for generating many tRNA halves, other as-yet unidentified endonucleases are also likely involved in their biogenesis¹⁶. Moreover, these tRHs are abundantly found in the extracellular milieu, demonstrating remarkable stability and resistance to degradation despite the presence of RNases^{17,18}. While the exact role of tRHs in biological fluids remains unclear, several researchers propose that these molecules may have paracrine or even endocrine functions¹⁹.

In recent times, the increased availability of sRNA-seq techniques has greatly enhanced our understanding of these molecules. It has become evident that the dysregulation of the levels of tRNA fragments carries substantial clinical implications across various pathologies²⁰. Of particular significance are those isolated from extracellular fluids, as this unveils novel possibilities for diagnosis and treatment.

In the context of asthma, different biofluids such as sputum, bronchoalveolar lavage fluid (BALF), and exhaled breath condensate (EBC) have been investigated for extracellular RNAs. While the predominant focus in research has been on the roles of microRNAs, long non-coding RNAs, and circular RNAs²¹, several reports indicate that these biofluids contain significant quantities of tRNA-derived fragments, similar to other human biofluids analyzed to date^{18,22–24}.

In this work, we investigated the role of ANG and tRHs in asthma using sputum and blood samples from patients, as well as in an *in vitro* model of pollutant-aggravated allergen stimulation. We observed a significant increase in ANG expression in circulating leukocytes of severe asthma patients, and altered levels of specific tRHs in both plasma and sputum, particularly 5'-tRH Glu and 5'-tRH Gly. Our findings highlight the dysregulation of these molecules in the course of asthma pathogenesis, suggesting their potential use as markers for asthma phenotyping.

Results

Systemic biomarkers for eosinophilic asthma cannot identify severe patients

To assess the precision of commonly employed markers for asthma phenotyping, we collected both sputum and blood samples from 40 patients: 13 healthy controls and 27 asthmatics, 13 of which were severe cases according to GINA guidelines. The characteristics of the population studied are depicted in Table 1. As previously described^{4,7,25,26}, eosinophils are elevated in patients compared to healthy controls while IgE levels show high dispersion samples resulting in no between-group differences (Fig. 1). Interestingly, only eosinophils in sputum could discriminate mild/moderate from severe asthmatics (Table 1) and their proportions did not correlate with those from blood (Supplementary Fig. 1). These findings further indicate that blood eosinophilia and atopy have poor prognostic value to classify asthmatic patients in severity and highlight the need for a deeper understanding of the disease to identify new tools.

Altered levels of ANG, 5'-tRH Gly and 5'-tRH Glu associates with severe inflammatory phenotypes

Recent findings highlighted ANG and tRH as novel key players in stress response and cell survival^{9,10}. In our cohort, we found that ANG expression is significantly increased in circulating leukocytes from patients with severe asthma, but not in inflammatory infiltrates from sputum (Fig. 2a, b). Similar results were obtained when we discriminated patients according to sputum inflammatory phenotype, where ANG in circulating leukocytes showed increased levels in those with eosinophilic infiltrates in sputum, a hallmark of severe patients (Fig. 2c–d). To validate these data, we conducted Western blot assays to assess protein levels. Our results demonstrated that ANG protein is predominantly localized in the extracellular space, with intracellular levels being negligible compared to those detected in plasma. Notably, ANG levels were significantly higher in patients compared to controls, aligning with the qPCR data (Supplementary Fig. 2).

Regarding tRNA derived fragments, we focused on those with potential applications as non-invasive biomarkers. In line with this goal, we looked for molecules highly abundant in fluids derived from the respiratory tract among those already described as potential targets of ANG. Our bioinformatic analysis based on sRNA-seq data from the Human Biofluid RNA Atlas²³, included only reads that aligned to the human genome. When specifically analyzing tRNA molecules, we found that 34.22% of the reads in samples of saliva, 31.78% in sputum and 4.76% in BAL aligned with this category. In all cases, more than 80% of the reads correspond to fragments of 4 tRNAs: Glu, Gly, Lys and Val (Fig. 3). Among them, we selected Glu and Gly for further studies. Fragments of these two tRNAs have been well-documented in extracellular fluids, including blood^{18,23,27}, and their quantification is highly reproducible and cost-effective.

Screening cohort	Healthy subjects n = 13	Patients with mild asthma n = 14	Patients with severe asthma n = 13
Demographic characteristics			
Age, median (min–max)	41 (27–64)	55 (24–68)	51 (26–76)
Sex (M/F)	7/6	6/8	6/7
IMC (Kg/m ²) mean ± SD	25.0 ± 3.13	31.6 ± 6.91	30.7 ± 7.66
Spirometry			
FEV1 (mL); median (min–max)	–	72.0 (46–96)	59.5 (24–85)
FEV1/FVC ratio; median (min–max)	–	88.0 (58.0–108)	82.5 (61.0–100)
Reversibility (%); median (min–max)	–	8.30 (–0.67–26.0)	7.80 (–3.90–25.8)
Blood leukocyte formula			
Lymphocyte (%); median (min–max)	33.0 (26–46)	27.5 (16–38)	32.0 (19–47)
Monocyte (%); median (min–max)	6 (3–10)	5.1 (3–9)	6.50 (3.3–13)
Neutrophils (%); median (min–max)	63.0 (40–66)	63.1 (51–79)	56.5 (47–65)
Eosinophils (%); median (min–max)	2 (1–4)	3.9 (2.4–16)	3.3 (2–7.2)
IgE; median (min–max)	139 (1.5–310)	172 (34–3050)	125 (29–1243)
Sputum characteristics			
Eosinophilic/neutrophilic/paucigranulocytic	2/6/5/0	5/4/3/2	8/2/0/3
Macrophages (%); median (min–max)	21.6 (5.8–40)	24 (6–57)	17.5 (7.7–34.3)
Neutrophils (%); median (min–max)	75.0 (54–93)	71.3 (36–93)	71.0 (56–89)
Eosinophils (%); median (min–max)	2.00 (0–8)	3.0 (0.5–6)	4.30 (1.6–29)(***)

Table 1. Clinical characteristics of the study groups. Data are presented as median (25–75 percentiles) unless otherwise specified. ***Statistically different from the Healthy group (Kruskal–Wallis analysis, followed by post-hoc test $p < 0.001$).

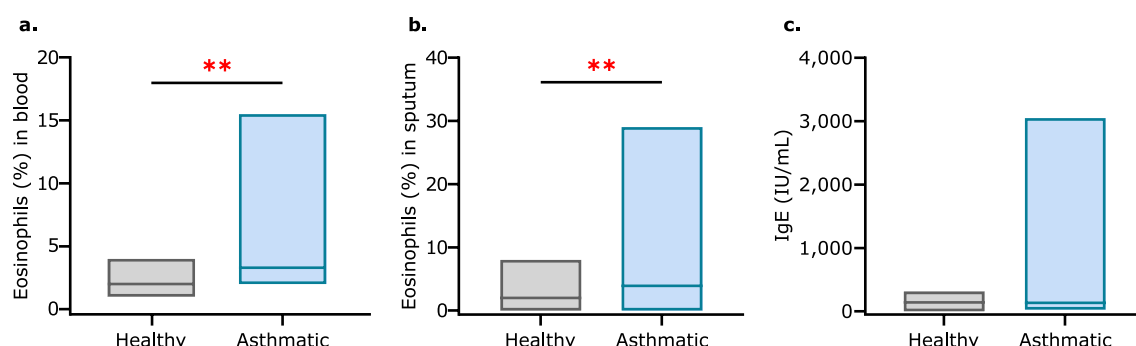


Fig. 1. Percent Eosinophil and IgE Levels in Asthmatic (n = 27) and Healthy Individuals (n = 13). Percent eosinophil in (a) blood and (b) sputum samples and (c) IgE levels in blood samples from both groups are shown. Box plots show maximum and minimum values in each group and the line represents the median values (** $p < 0.01$, Mann–Whitney U test).

To better characterize the diversity of fragments derived from the selected tRNAs and identify consensus sequences, we generated sequence logos for Gly and Glu fragments using all reads assigned to these tRNAs in each sRNA-seq experiment. We then compared results across different datasets (Fig. 3b). For these analyses, we focused on sputum and blood samples with the aim of identifying potential biomarker candidates. Specifically, we use two sputum datasets from the Human Biofluid RNA Atlas and serum samples from 9 independent experiments with publicly available raw data^{23,28,51–57}. As shown in Fig. 3b, the majority of sequences detected in both biofluids correspond to 5' tRNA halves. Table SII compiles all the sequences assigned as tRNA Gly and Glu, along with their relative abundance in each analyzed sample.

To verify the presence of these sequences in the selected biofluids, we conducted Northern blot analysis. As shown in Fig. 3c, while both full-length tRNAs and 5' fragments are readily detectable in cells, their abundance in extracellular fluids is markedly reduced. Only a ~30 nt fragment, corresponding to the 5' tRNA fragment, was observed in some samples.

For subsequent quantification studies using qPCR, we defined representative sequences for each fragment, prioritizing those with the highest relative abundance and consistent detection across different datasets. Their names were assigned using the MINTmap tool²⁹, identifying the sequences as 5'-tRH Glu (tRF-32-87R8WP9N1EWJM) and 5'-tRH Gly (tRF-30-PNR8YP9LON4V). To evaluate the role of these molecules in asthma we quantified both tRHs in sputum and blood samples of asthmatic patients. Their levels were assessed

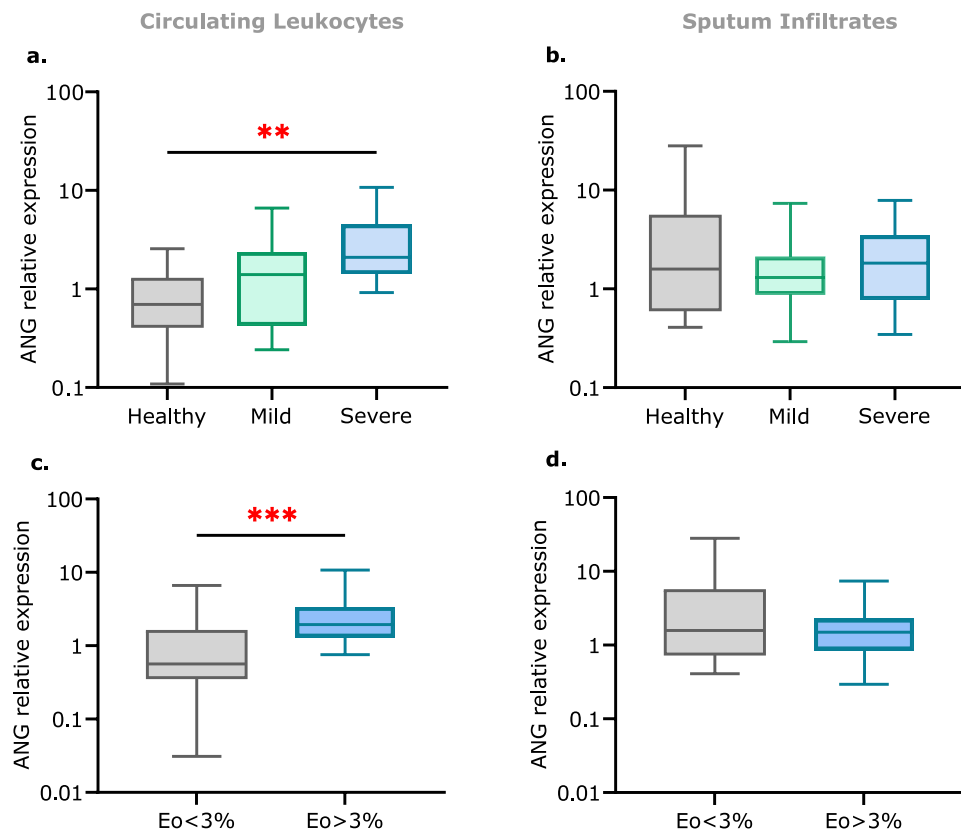


Fig. 2. Relative expression of ANG in sputum and blood samples from asthmatic patients. Quantification of the ANG transcript in (a) circulating leukocytes and (b) sputum infiltrates in asthmatic patients (mild = 14, severe = 13) and a control group (n = 13) stratified by GINA guidelines. Alternative analysis on asthmatic patients based on sputum inflammatory phenotype stratification (Eo < 3% = 9, Eo > 3% = 18) is shown in (c) circulating leukocytes and (d) sputum infiltrates. Data are presented as box plots showing the interquartile range, with whiskers indicating the minimum to maximum values, and the line representing the median (** $p < 0.01$, Kruskal–Wallis test (panel a), *** $p < 0.001$, Mann–Whitney U test (panel c)).

both in cells obtained from the sample (leukocytes) and in extracellular fluids. Figure 4 shows that tRHs expression is not altered either in blood or in sputum cells. However, we found that their levels are significantly altered in extracellular fluids from asthmatic patients. Both tRHs are strongly downregulated in plasma while in sputum, 5'-tRH Gly levels are significantly elevated in severe cases, with 5'-tRH Glu showing a trend to higher levels in these patients (Fig. 4 and Supplementary Fig. 3). In both tissues, the lack of correlation with what is observed in cells indicates that tRHs levels in the extracellular space are unlikely to result from cell lysis.

Although full-length tRNAs are highly unlikely to be amplified using SLO-RT-qPCR due to steric constraints that prevent reverse transcription of intact tRNAs, we acknowledge that the technique may also amplify fragments with one or two additional nucleotides at the 3' end. sRNA-seq data confirm that these sequences are indeed present in the samples. Different lines of evidence suggest that these families of related sequences are generated through exonucleolytic trimming of tRHs initially produced by cleavage from type-A RNases, such as ANG¹³. Consequently, the results presented in this manuscript should be interpreted with the understanding that the quantifications reflect the cumulative levels of multiple variants of the same tRH.

The ANG/tRHs axis is induced in DEP-enhanced, allergen-stimulated macrophages

Since macrophages are the first line of defense in lung tissue, we also tested ANG and tRHs expression in the THP1 cell line. Cells were allergen-stimulated with extracts of *D. pteronyssinus* (HDM) and the immune response was enhanced using particulate matter produced by diesel engine exhaust (DEP). In this model, we observed a strong activation of macrophages with a hybrid bias, characterized by the production of cytokines typical of both M1 and M2 profiles (Supplementary Fig. 4). Our results are depicted in Fig. 5 and show that 24 hs treatment with DEP, either alone or combined with HDM induce ANG expression and increase extracellular levels of 5'-tRH Glu and 5'-tRH Gly, with no changes in their expression within the cells. To further validate these findings, we quantified both tRNA halves at shorter time points (4 and 12 hs) and also observed a significant increase in their levels in the supernatants of cells treated with DEP and DEP/HDM across both experiments (Supplementary Fig. 5). Additionally, we conducted Western blot analysis to assess protein levels of ANG in THP-1 cells after a 24 hs treatment, confirming a slight increase in ANG levels in DEP-treated cells (Supplementary Fig. 6). These findings are in agreement with results obtained in vivo with severe asthmatic patients.

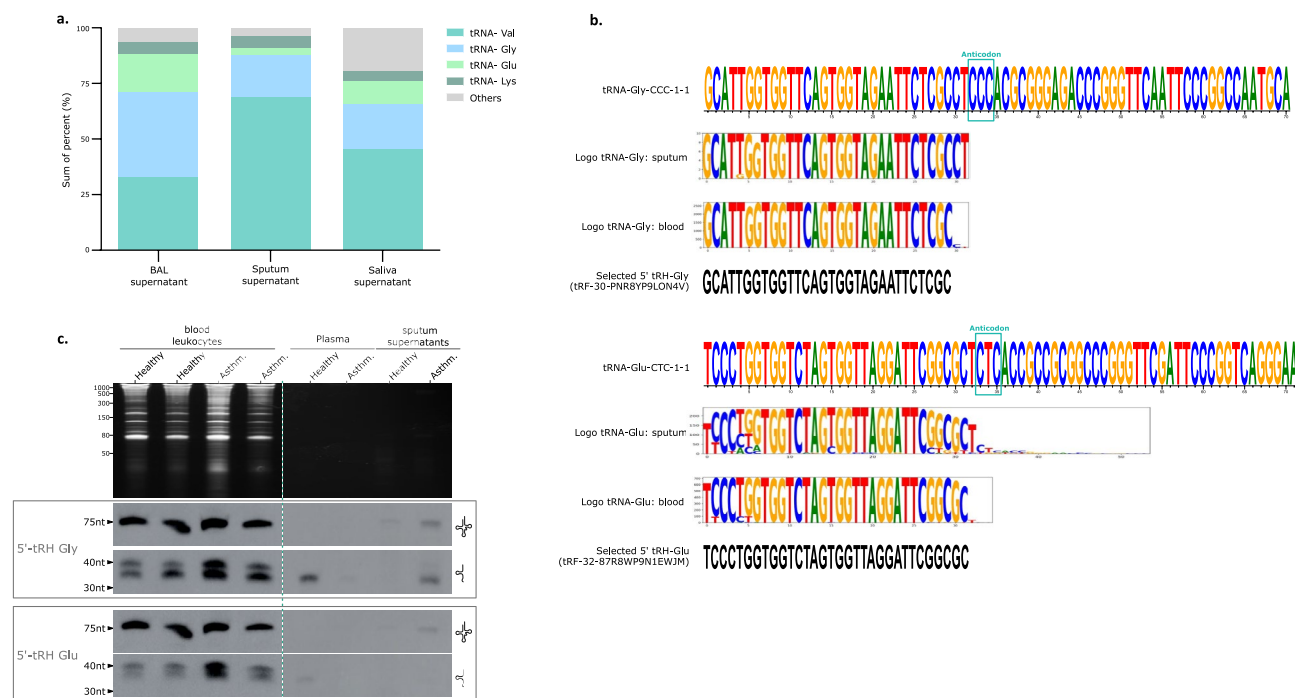


Fig. 3. Characterization of tRNA derived fragments highly abundant in biofluids. Percentage distribution of tRNAs in bronchoalveolar lavage (BAL), sputum, and saliva samples (a). Sequence logo of tRNA fragments derived from tRNA Glu and tRNA Gly. The fragments are mapped to the closest corresponding reference tRNAs. tRNA halves (tRHs) selected for qPCR analysis are highlighted (b). Northern blot analysis of tRNA Gly and tRNA Glu in blood leukocytes, plasma, and sputum supernatant samples from patients (severe asthmatic and healthy controls). Probes specific to 5'-tRH Gly and 5'-tRH Glu were used to detect the corresponding tRNA fragments (c). Blots were cropped for clarity, with original images available in Supplementary Fig. 8.

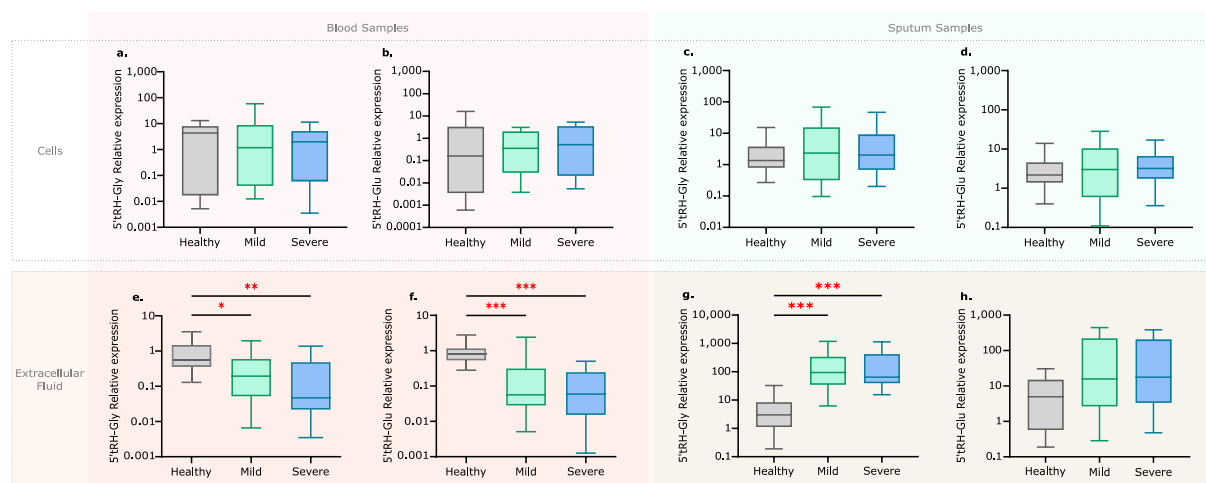


Fig. 4. Quantification of tRHs in sputum and blood samples from asthmatic patients. Relative expression of 5' tRH-Gly and 5' tRH-Glu in blood leukocytes (a and b) and in sputum infiltrates (c and d). Extracellular levels were determined in plasma (e and f) and sputum supernatants (g and h) using spike-in cel-miR-39 as the exogenous control. The data are normalized to the healthy group, and quantifications were conducted using Stem Loop RT-qPCR. Data are presented as box plots showing the interquartile range, with whiskers indicating the minimum to maximum values, and the line representing the median (* $p < 0.05$, ** $p < 0.01$, *** $p < 0.001$, Kruskal–Wallis test).

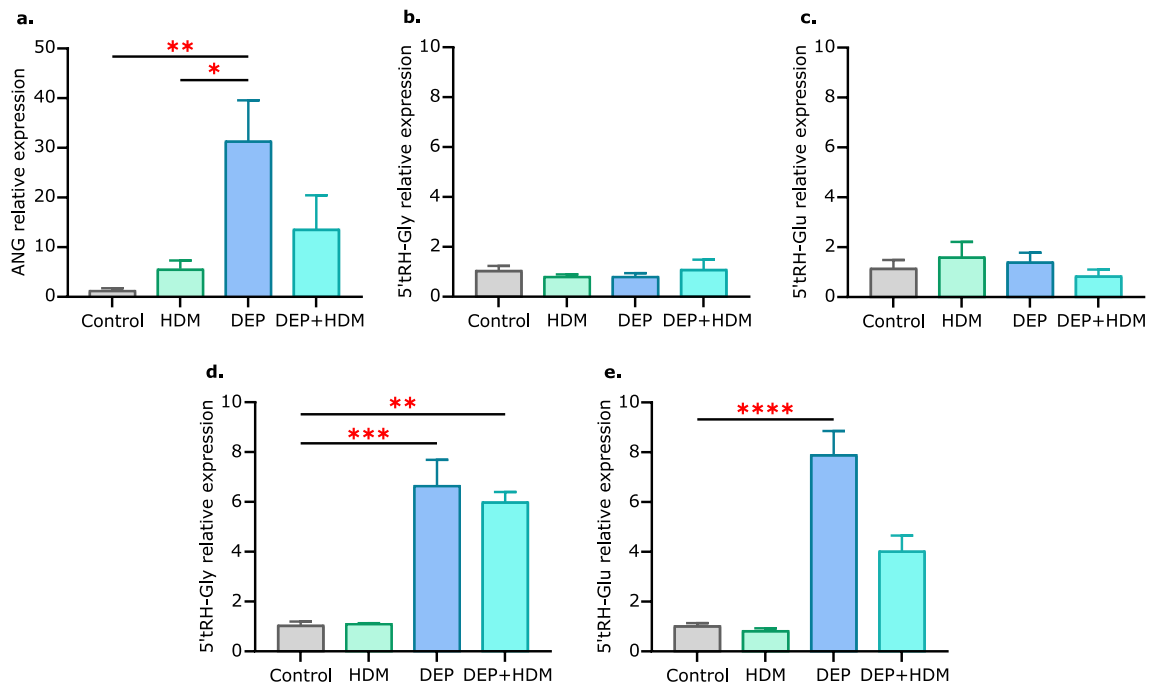


Fig. 5. Levels of ANG and tRHs in DEP-enhanced, allergen-stimulated macrophages. THP-1 cells were treated with DEP, HDM, or a combination of both agents. Quantification of (a) ANG, (b) 5'-tRH Gly, and (c) 5'-tRH Glu in cells, and (d) 5'-tRH Gly, and (e) 5'-tRH Glu in cell culture supernatant was performed by Stem Loop RT-qPCR. Data are presented as mean \pm SEM of 4 biological replicates (* p < 0.05, ** p < 0.01, *** p < 0.001, and **** p < 0.0001, one-way ANOVA test followed by post hoc comparisons when applicable).

Disrupted adrenal response in severe asthma shows an inverse correlation with tRH production

Considering the crucial role of corticosteroid response in asthma regulation, we examined its potential correlation with ANG and tRH levels, as both mechanisms aid in stress adaptation. First, we quantified plasma cortisol and the expression of the glucocorticoid receptor (GR) in blood cells in our cohort. Figure 6a and b show that cortisol levels in severe asthma patients are significantly lower than those in healthy controls, while GR expression remains stable. We also measured the expression of histone deacetylase 2 (HDAC2), a key enzyme in epigenetic modifications associated with corticosteroid responsiveness. Although HDAC2 levels in blood cells remained unaltered when comparing healthy individuals and patients (Fig. 6c), they showed a strong correlation with GR expression (Fig. 6d). Similarly, we found a highly significant negative correlation between GR levels and tRH levels produced by circulating leukocytes (Fig. 6e,f). Collectively, our findings suggest a mechanistic link between these regulatory pathways. No associations were observed between ANG or extracellular tRHs and any of the mediators of the corticosteroid response, either in circulation or in sputum samples.

To further characterize the GR expression in the lung, we employed a murine model of pollution enhanced allergic airway inflammation. In this previously published model, concomitant exposure of mice to diesel exhaust particles (DEP) and house dust mite (HDM) significantly enhances allergic airway inflammation, type 2 cytokine production, airway eosinophilia and goblet cell metaplasia compared to control groups exposed to HDM, DEP or saline³⁰. Using this model we found that GR mRNA expression is significantly lower in the lungs from mice treated with DEP, either alone or in combination with HDM compared to saline (Fig. 7a). Immunolocalization assays showed that GR was mainly localized in bronchial epithelial cells (Fig. 7b-c (mice) and Supplementary Fig. 7 (humans)). Unfortunately, the available material was insufficient to proceed with tRH quantification using the SLO RT-qPCR technique. However, recent studies conducted by Shigematsu et al. showed elevated levels of both tRHs in the lung tissue of HDM-sensitized mice³¹, in agreement with our findings in human samples.

Discussion

This study delved into the complex landscape of asthma, shedding light on previously unexplored pathways involving the production and secretion of tRNA fragments in the progression of this condition at both systemic and local levels. Our key findings reveal a significant upregulation of ANG expression in circulating leukocytes of severe asthma patients, alongside notable alterations in the extracellular levels of 5'-tRH Glu and 5'-tRH Gly in both blood and sputum samples from individuals with asthma. These results are further supported by in vitro experiments using allergen-stimulated macrophages, suggesting a conserved mechanism across various cell types. Overall, the present findings identify soluble mediators in both blood and pulmonary secretions that hold promise for applying liquid biopsies in characterizing clinical phenotypes of asthma.

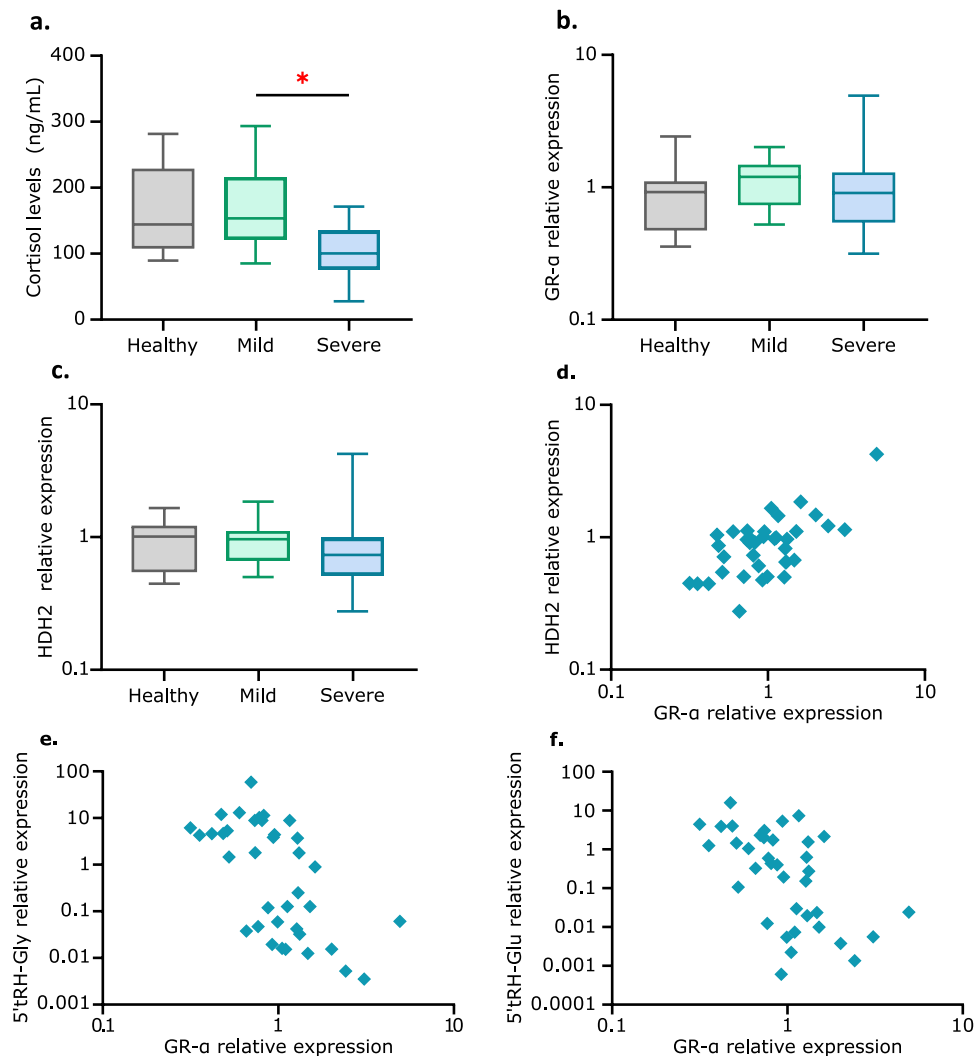


Fig. 6. Levels of circulating cortisol, GR-α, and HDAC2 in blood samples of asthmatic patients and healthy individuals. Quantification of plasmatic cortisol (a), and relative expression of GR-α (b) and HDAC2 (c) in blood leukocytes of healthy ($n = 13$), mild ($n = 14$), and severe ($n = 13$) asthmatic patients. Box plots show the interquartile range, with whiskers indicating the minimum to maximum values, and the line representing the median (* $p < 0.05$, Kruskal–Wallis test). (d) Spearman correlation ($R = 0.5377$, $p = 0.0006$) between GR-α and HDAC2 transcripts. (e) and (f) Spearman correlation between GR-α and circulating levels of 5' tRH-Gly ($R = -0.6172$, $p = 0.0001$) and 5' tRH-Glu ($R = -0.5477$, $p = 0.0005$).

Severe asthmatic patients pose a significant clinical challenge due to their resistance to standard corticosteroid therapy. It has been observed that these patients exhibit an inadequate or dysfunctional response to environmental and physiological stressors, which can exacerbate inflammation and airway obstruction³². These disruptions in stress response mechanisms may trigger acute asthma exacerbations, escalating the severity of the disease and compromising the patient's quality of life. Effective diagnostic tools are crucial for the correct management of severe asthmatic patients. However, commonly used markers for asthma phenotyping lack sufficient prognostic value in classifying these patients. In our study, we offer additional data demonstrating that blood eosinophilia and atopy are insufficient for discriminating severe cases.

Emerging evidence indicates that changes in expression patterns of tRNA derived fragments are associated with the pathogenesis of stress-related disorders^{33–36}. These molecules are hypothesized to serve as an ancestral mechanism for cell survival, and their elevated levels in extracellular fluids suggest their involvement in intercellular communication^{37–39}. To initiate the characterization of these mechanisms in asthma, we quantified the levels of ANG, a well known ribonuclease responsible of generating tRHs, and 5' tRH Glu and 5' tRH Gly, two tRHs highly abundant in biofluids. We assessed these in both blood and sputum samples collected from healthy individuals and asthmatic patients with varying degrees of severity.

These molecules were selected based on a bioinformatic analysis conducted in our laboratory, analyzing publicly available sRNA seq data from sputum, saliva, and BAL samples²³. The tRNA-derived fraction in these samples mainly comprised tRHs derived from GLU, GLY, LYS, or VAL. These findings align with existing

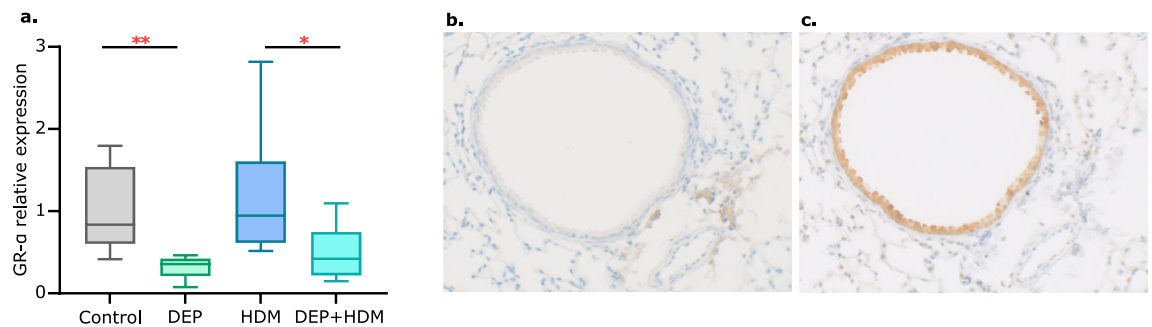


Fig. 7. (a) Quantification of mRNA levels for the glucocorticoid receptor (GR) transcript in a murine model of asthma exacerbated by pollution. Mice were exposed to 1 μ g house dust mite (HDM), 25 μ g diesel exhaust particles (DEP), and a combination of both (DEP + HDM) ($n = 6$). (b and c) Representative photomicrographs of Immunolocalization of the GR α isoform in the lungs of mice. (b) Isotype control and (c) Immunostaining of airways at 20 \times magnification. Tissues were counterstained with hematoxylin (blue). Data from panel a are presented as box plots showing the interquartile range, with whiskers indicating the minimum to maximum values, and the line representing the median (* $p < 0.05$, ** $p < 0.01$ Kruskal–Wallis test).

literature describing these fragments as highly abundant in blood and other analyzed biofluids^{18,40}. Among them, we chose 5'-tRH Glu and 5'-tRH Gly due to their documented enhanced stability in extracellular fluids. This stability arises from their capacity to form various secondary structures, acting as stable reservoirs in the extracellular space^{27,41}.

It is important to note that, in theory, 5' tRNA fragments should not be detected in standard sRNA-seq due to their 5'-phosphate (5'-P) and 3'-cyclic phosphate (3'-cP) ends, which prevent adaptor ligation. However, in practice, they are frequently observed, likely due to exonucleolytic trimming that modifies these termini. Recent studies have shown that treatment with T4 polynucleotide kinase (T4 PNK) significantly enhances the representation of tDRs in RNA-seq libraries by enabling adaptor ligation⁶⁹. These findings suggest that advanced methods like cP-RNA-seq or PANDORA-seq should be employed in future studies to achieve a more unbiased view of tDR diversity.

The results obtained in this study indicate that the ANG/tRHs pathways are disrupted in asthmatic patients. Our analysis of blood samples revealed an elevated expression of ANG in circulating leukocytes of severe patients compared to other groups, which did not correlate with alterations in the levels of tRHs in these cells. Our western blot results indicate that ANG protein is primarily localized in the extracellular space, suggesting that it is predominantly secreted. Given that ANG's functionality depends on its cellular localization—with its active ribonuclease activity primarily occurring in the cytoplasm—we hypothesize that the elevated levels of ANG observed in asthmatic patients could be linked to its other documented roles, such as antimicrobial activity and tissue regeneration, which may be relevant in the context of the disease⁴³. On the other hand, quantification of both 5'-tRHGly and 5'-tRH Gly in plasma revealed a highly significant downregulation of these molecules in asthmatic patients, regardless of their severity.

When analyzing the patterns of these markers in sputum, we observed a notable divergence compared to what was observed in blood. RNA extracted from cells obtained from this secretion showed no differences in the expression of either ANG or the tRHs across the study groups. However, extracellular levels of tRHs were elevated in sputum supernatants from severe patients, with tRH Gly reaching statistical significance. In line with this evidence, a recent article from Shigematsu et al. showed that both tRHs are elevated in the lungs of HDM-treated mice³¹.

It is noteworthy that there is a lack of correlation between intra- and extracellular tRH levels in both types of samples analyzed, indicating that the data obtained from extracellular fluids cannot be attributed to cell lysis during sample processing. These findings suggest that the cells lining the barriers of these fluids may be responsible for secreting tRHs into the extracellular environment. Evidence supporting this view comes from studies in seminal fluids, where it has been observed that epididymal epithelial cells actively release sRNA during the maturation process of spermatozoa⁴⁴. Aligned with this hypothesis, we investigated the effects of environmental stress on allergen-stimulated macrophages, given their pivotal role in defending and maintaining the homeostasis of all barrier epithelia. Our results showed that treatment with DEP, either alone or combined with HDM induces ANG expression and increases extracellular levels of 5'-tRH Glu and 5'-tRH Gly. This further validates the data obtained from both human sputum samples and animal models.

Finally, we delved into the correlations between adrenal response and ANG/tRH levels in asthmatic patients, aiming to assess potential synergies between cellular and systemic stress responses. The interplay between ANG, tRFs, and glucocorticoids could provide additional layers of regulation to fine-tune the stress response and control inflammation. For instance, specific tRFs have been shown to activate p65, a key component of the NF- κ B signaling pathway⁴⁵. Additionally, other studies have demonstrated that 5'-tRHs can activate Toll-like receptor 7 (TLR7), which is crucial for initiating immune responses^{46,47}. Within our study cohort, we observed significantly lower cortisol levels in severe patients compared to healthy controls. These findings may be attributed to the induction of a hyporesponsive state of the HPA axis (i.e., relative deficiency), potentially stemming from exacerbated cytokine production (chronic inflammation may also account for such disturbance)³². Alternatively,

it could result from negative feedback on the axis due to the use of inhaled corticosteroids at higher average doses in severe patients compared to mild/moderate cases (patients on oral corticosteroids were excluded from the study). Further evidence of a mechanistic link between these pathways during the course of the disease is demonstrated by our findings of an inverse correlation between tRH and GR levels in our cohort. Additionally, studies in mice revealed that pulmonary remodeling triggered by environmental stress results in an overall reduction in GR expression within the tissue. Taken together, our results provide additional evidence that the corticosteroid response is deficient in severe asthma cases, characterized by lower levels of circulating cortisol and reduced bioavailability of GR in the lungs, likely due to tissue remodeling. This adrenal disruption is associated with ANG/tRH pathways throughout the course of the disease.

In sum, our study underscores the association between altered levels of extracellular tRHs and asthma, although contrasting data emerged from plasma and sputum supernatants. In plasma, we observed a significant decrease of both 5'-tRH Glu and 5'-tRH Gly in samples from asthmatic patients, whereas in sputum supernatants, they appeared to be overexpressed only in severe cases. This discrepancy provides a stimulating background for further investigation, particularly the role of these molecules in extracellular fluids, which remains unexplored to date. Nevertheless, the consistency of our findings, both within our study and in relation to existing literature, suggests a potentially pivotal role of these molecules in the pathogenesis of asthma. Further appraisal of the intricate roles played by tRNA fragments will deepen our understanding of cellular stress responses and may pave the way for the development of innovative strategies to mitigate complex pathologies such as asthma.

Material & methods

Study groups

All methods were performed in accordance with the relevant guidelines and regulations, including the Declaration of Helsinki. Participants were recruited at CIC-IESR, Argentina and after signing a written informed consent form, they were asked to provide a sputum and blood sample. All experimental procedures and methods performed in this work were approved by the Ethical and Biosafety Committees from the School of Medical Sciences of Rosario National University (resolution N° 6192/2018). The study population consisted of healthy subjects ($n=13$), patients with mild-to-moderate asthma ($n=13$), and patients with severe asthma ($n=14$). Table 1 provides an overview of the demographic, functional, and treatment characteristics of the subjects. Asthma severity was evaluated by a respiratory physician based on a combination of symptoms, lung function, and amount of medication to achieve control¹. Severe asthma required GINA treatment steps 4 to 5. All subjects were nonsmokers (never smokers or ex-smokers who quit smoking for at least 6 months).

Blood samples were collected between 8 and 9 am before sputum induction and employed for routine laboratory assays. Additionally, plasma samples were collected and preserved at -70°C for Cortisol quantification and RNA extraction. White blood cells were isolated from EDTA-treated samples using a standard protocol (RBC lysis buffer + centrifugation) and preserved at -70°C for RNA extraction.

Sputum induction

Sputum was induced and processed, as described previously⁴⁸. Whole sputum was weighted, and 4 volumes of 0.1% DTT-PBS were added. After vigorous homogenization for 15 min, 4 more volumes of PBS were added and samples were centrifuged (1400 g) for 10 min at 4°C . Then, the cell pellet and supernatant were separated and stored at -70°C . Asthma inflammatory phenotype was defined by counting 300 sputum cells on cytopspin samples stained with Hematoxylin–Eosin and MayGrunwald-Giemsa. Eosinophilic asthma was defined as $\geq 3\%$ of sputum eosinophils and less than 76% sputum neutrophils, whereas neutrophilic asthma was defined as $\geq 76\%$ of neutrophils and less than 3% eosinophils. Criteria for paucigranulocytic asthma were less than 3% and 76% of and mixed granulocytic $\geq 3\%$ and $\geq 76\%$ of eosinophils and neutrophils, respectively.

Hormone assessment

Circulating Cortisol (DRG Instruments GmbH) concentrations were assessed according to the manufacturer's instructions. All samples were processed individually and assayed in duplicate. The detection limit was 1.3 ng/ml.

RNA isolation and RT-qPCR

Total RNA from leukocytes ($1-3 \times 10^6$ cells) and cell-free supernatants (200 μL) was isolated using TRI-Reagent (MRC Inc., Toledo, OH, USA) according to the manufacturer's recommendations. cDNA was synthesized using Superscript III reverse transcriptase (Thermo Fisher Scientific, MA, USA) and PCR reactions were performed in a StepOne Real-Time PCR System (Thermo Fisher Scientific, MA, USA) using HOT FIREpol EvaGreen Plus master mix (Solys Biodyne, Estonia). Small RNA levels were determined using an adaptation of the stem-loop RT-qPCR technique previously established in our lab, modified to use SYBR instead of TaqMan probes^{49,50} (List of primers employed in this work is depicted in Suppl. Table I). PPIA and U6 snRNA were employed for mRNA and sRNA normalization in cell extracts, respectively. Normalization of samples derived from extracellular fluids was performed using spike-in cel-miR-39 as the exogenous control. Additional data supporting the tRH quantification method are provided in Supplementary Fig. 10.

GR expression in the murine model of pollutant-aggravated allergic asthma

The model developed at the Department of Respiratory Medicine (Ghent University, Belgium) involves challenging mice with house dust mite (HDM), diesel exhaust particles (DEP) and a combination of both irritant agents³⁰. All in vivo manipulations were approved by the Animal Ethical committee of the Faculty of Medicine and Health Sciences of Ghent University (approval code ECD 12/59) and were performed according to the ARRIVE guidelines. All methods were also performed in accordance with the relevant guidelines and

regulations. The wellbeing of the animals was recorded with a score-sheet, evaluating body condition, appearance, natural behavior, hydration and respiration. The humane endpoints registered in ECD 12/59 were: if animals show signs of suffering such as reduced physical activity, abnormal coat condition or posture or reduction of body weight with more than 20%, the experiment will be prematurely terminated. However, the experimental procedures in the model only led to a very short moment of stress, thus none of the mice reached the humane endpoints. Saline, 1 µg of HDM extract dissolved in saline, 25 µg of DEPs suspended in saline, or a combination of DEP + HDM was delivered intranasally to isoflurane-anesthetized mice by using a continuous flow vaporizer on days 1, 8, and 15. Two days after the last challenge, mice were killed with a lethal dose of intraperitoneal pentobarbital.

cdNA samples and lung tissue sections from experiments depicted in De Grove et al.³⁰ were employed in this work. GR mRNA levels were determined as described above.

For immunolocalization assays, sections were deparaffinized and rehydrated with xylene and alcohol gradient. After antigen retrieval (citrate, 90 °C, 45 min) and blocking, samples were incubated overnight (4 °C) with primary polyclonal antibody against GRα (Thermo Scientific cat #PA1-516) or Isotype negative control (rabbit Ig (Novus #NB810-56910). Anti rabbit-HRP secondary antibody (Klinipath DPVR-55HRP) and DAB reagent (DAKO #K3468) were used for detection. Sections were counterstained with hematoxylin.

Bioinformatic analysis

sRNA-seq data of sputum, bronchoalveolar fluids (BAL), saliva and serum samples were obtained from the Human Biofluid RNA Atlas of Hulstaert et al.²³. Serum samples from 8 publicly available dataset were also employed (GSE113994, GSE90028, GSE156874, GSE151963, GSE126051, GSE90524, GSE158312, GSE71579)^{28,51–57}. Samples were processed using a custom pipeline built in Python 3.10. Fastq files corresponding to the dataset were downloaded from the European Genome-Phenome Archive (EGA—EGAS00001003917) with permission from the corresponding authors. Files were quality-controlled following standard procedures. Briefly, sequencing adapters were trimmed using cutadapt, known contaminants were filtered using the UNIVeC database and FASTQC 0.11.9⁵⁸ was used for quality control. Sequences were then assigned by performing a series of alignments. First, bowtie2 2.4.4⁵⁹ was used on the on the ‘-very-sensitive-local’ preset –score-min L,0,1 to align all sequences to curated reference sequences for tRNA (gtRNAdb⁶⁰), rRNA (rFAM⁶¹, RNACentral), miRNA (mirBASE⁶²) and yRNA. The remaining sequences were aligned to the reference human genome (GRCh38) using HISAT2 2.2.1⁶³. Bedtools 2.30.0⁶⁴ intersect was used to extract the annotations for matching fragments from the corresponding annotation file. All statistics and visualizations related to sRNA-seq data were built by analyzing the results in Pandas and visualizing with Plotly. Sequence logos were performed as described in Schneider and Stephens, 1990. In these graphs, the X-axis denotes the position in the sequence, The height of each letter is made proportional to its frequency, and the letters are sorted so the most common one is on top. To account for the relative abundance of each sequence, this analysis applied a weighting factor proportional to the percentage of reads corresponding to each sequence relative to the total read count in each sample. The height of the entire stack is then adjusted to signify the information content of the sequences at that position⁶⁵. For downstream quantification studies using qPCR, we defined representative sequences of each fragment and assigned their names using the MINTmap tool^{29,66}.

Cell culture

The THP1 cell line was purchased from ATCC, and authenticity was documented by standard STR analysis. Cells were grown in suspension cultures in RPMI 1640 medium supplemented with 10% FBS and 100 units/ml penicillin and streptomycin (Invitrogen) at 37 °C in 5% CO₂. For differentiation to macrophages, cells were plated in 12-well dishes (1 × 10⁶ cells per well) on RPMI containing 10 ng/ml phorbol-12- myristate-13-acetate (PMA, Sigma Chemical Co) were used as a model of undifferentiated (M0) macrophages. After 24 hs, supernatants were removed and complete RPMI was added for 48 hs before treatment. THP-1 cells were exposed to extracts of house dust mite (HDM; *Dermatophagoides pteronyssinus*) at 50 AU, with particulate matter produced by diesel engine exhaust, (DEP kindly donated by Dr. Berra⁶⁷ at 50 µg/ml and with a combination of both treatments. Cells and culture supernatants were collected after 4, 12 and 24 hs of treatment for quantification of transcripts and sRNAs by SLO-RTqPCR.

Northern blotting

RNA samples were run on 10% TBE-urea polyacrylamide gels, transferred to positively charged nylon membranes (Roche). For each lane, RNA purified from 200 µL of biofluid (sputum or serum) was loaded, while 1 µg of RNA was used for cellular controls. The membranes were cross-linked by UV irradiation. After cross-linking, the membranes were hybridized overnight at 40 °C with digoxigenin (DIG)-labeled DNA probes in DIG Easy Hyb solution (Roche). After low stringency washes (washing twice with 2 × SSC/0.1% SDS at room temperature) and a high stringency wash (1 × SSC/0.1% SDS at 40 °C), the membranes were blocked in blocking reagent (Roche) for 30 min at room temperature, probed with alkaline phosphatase-labeled anti-digoxigenin antibody (Roche) for 30 min, and washed with 1 × TBS-T. Signals were visualized with CDP-Star ready-to-use (Roche) and detected using Amersham Imager 600 (GE HealthCare) according to the manufacturer's instructions. Oligonucleotide probes were synthesized by IDT. DIG-labeled probes were prepared using the DIG Oligonucleotide tailing kit (2nd generation; Roche) according to the manufacturer's instructions. The sequences of the probes were as follows: 5'-tRH Gly: 5' CTACCACTGAACCAATGC 3'; and 5'-tRH Glu: 5' TAACCACTAGACCACCAG GGA 3'.

Western blotting

Serum protein extracts (protein concentrations ranging from 98 to 276 mg/ml) were prepared by diluting samples 1/40 with 1× Sample buffer. Extracts from whole blood cells and THP-1 cell cultures were obtained from 1×10^6 cells using 200 µL of RIPA buffer, followed by dilution with 1× Sample buffer. Samples were separated by 15% SDS-PAGE, and proteins were transferred onto nitrocellulose membranes. Membranes were blocked with 5% PBS-BSA for 1 h at room temperature and incubated overnight at 4 °C. For loading, 20 µL of 1/40 diluted serum and 30 µg of protein from cellular extracts (whole blood cells or THP-1 cells) were loaded per lane. The following primary antibodies were used: monoclonal anti-Angiogenin 1 (sc-74528, Santa Cruz) and polyclonal anti-β-actin (A2066, Sigma). HRP-conjugated anti-rabbit (111-035-003, Jackson) and HRP-conjugated anti-mouse (115-035-003, Jackson) secondary antibodies were applied. Chemiluminescence was detected using the Amersham ECL Prime Western Blotting Detection Reagent (GE Healthcare). In THP-1 experiments, membranes were cut to measure both primary antibodies during blotting. For quantitative analysis, Western blot band intensities were measured with ImageJ software⁶⁸ and normalized to their corresponding β-actin bands.

Statistical analysis

Comparisons between groups and compartments were performed using nonparametric methods, such as the Kruskal-Wallis analysis of variance (followed by post-hoc comparisons when applicable) and the Wilcoxon rank test. Correlations between variables were analyzed by Spearman's rank test. ANOVA test was employed to analyze data from THP-1 cell culture experiments. A *P*-value < 0.05 was considered statistically significant. All data were analyzed using GraphPad Prism 9.2.1 (San Diego, CA, USA) software.

Data availability

All data generated during this study are included in this published article (and its supplementary information files).

Received: 24 June 2024; Accepted: 20 May 2025

Published online: 29 May 2025

References

- Global Initiative for Asthma. *Global Strategy for Asthma Management and Prevention* (2023).
- Al Heialy, S., Ramakrishnan, R. K. & Hamid, Q. Recent advances in the immunopathogenesis of severe asthma. *Allergy Clin Immunol* **149**, 455–465 (2022).
- Guida, G. et al. Critical evaluation of asthma biomarkers in clinical practice. *Front. Med.* **9**, 969243 (2022).
- Diamant, Z. et al. Toward clinically applicable biomarkers for asthma: An EAACI position paper. *Allergy* **74**, 1835–1851 (2019).
- Gans, M. D. & Gavrilova, T. Understanding the immunology of asthma: Pathophysiology, biomarkers, and treatments for asthma endotypes. *Paediatr. Respir. Rev.* **36**, 118–127 (2020).
- Barnes, P. J. Glucocorticosteroids. *Handb. Exp. Pharmacol.* **237**, 93–115 (2017).
- Wadhwa, R. et al. Cellular mechanisms underlying steroid-resistant asthma. *Eur. Respir. Rev.* **28**, 190096 (2019).
- Ramos-Ramírez, P. & Tliba, O. Glucocorticoid insensitivity in asthma: The unique role for airway smooth muscle cells. *Int. J. Mol. Sci.* **23**, 8966 (2022).
- Lyons, S. M., Fay, M. M., Akiyama, Y., Anderson, P. J. & Ivanov, P. RNA biology of angiogenin: Current state and perspectives. *RNA Biol.* **14**, 171–178 (2017).
- Kumar, P., Kuscu, C. & Dutta, A. Biogenesis and function of transfer RNA-related fragments (tRFs). *Trends Biochem. Sci.* **41**, 679–689 (2016).
- Muthukumar, S., Li, C. T., Liu, R. J. & Bellodi, C. Roles and regulation of tRNA-derived small RNAs in animals. *Nat. Rev. Mol. Cell Biol.* **25**, 359–378 (2024).
- Xie, Y. et al. Action mechanisms and research methods of tRNA-derived small RNAs. *Signal Transduct. Target. Ther.* **5**, 1–9 (2020).
- Tosar, J. P. et al. Fragmentation of extracellular ribosomes and tRNAs shapes the extracellular RNAome. *Nucleic Acids Res.* **48**, 12874–12888 (2020).
- Sheng, J. & Xu, Z. Three decades of research on angiogenin: a review and perspective. *Acta Biochim. Biophys. Sin.* **48**, 399–410 (2016).
- Balatti, V., Pekarsky, Y. & Croce, C. M. Role of the tRNA-derived small RNAs in cancer: New potential biomarkers and target for therapy. *Adv. Cancer Res.* **135**, 173–187 (2017).
- Su, Z., Kuscu, C., Malik, A., Shibata, E. & Dutta, A. Angiogenin generates specific stress-induced tRNA halves and is not involved in tRF-3-mediated gene silencing. *J. Biol. Chem.* **294**, 16930–16941 (2019).
- Pardini, B., Sabo, A. A., Birolo, G. & Calin, G. A. Noncoding RNAs in extracellular fluids as cancer biomarkers: The new frontier of liquid biopsies. *Cancers* **11**, 1170 (2019).
- Godoy, P. M. et al. Large differences in small RNA composition between human biofluids. *Cell Rep.* **25**, 1346–1358 (2018).
- Dhahbi, J. M. 5' tRNA Halves: The next generation of immune signaling molecules. *Front. Immunol.* **6**, 74 (2015).
- Yu, X. et al. tRNA-derived fragments: Mechanisms underlying their regulation of gene expression and potential applications as therapeutic targets in cancers and virus infections. *Theranostics* **11**, 461–469 (2021).
- Stachowiak, Z., Narożna, B. & Szczepankiewicz, A. Non-coding RNAs in pulmonary diseases: Comparison of different airway-derived biosamples. *Int. J. Mol. Sci.* **24**, 2006 (2023).
- Li, F. et al. Characterization of human salivary extracellular RNA by next-generation sequencing. *Clin. Chem.* **64**, 1085–1095 (2018).
- Hulstaert, E. et al. Charting extracellular transcriptomes in the human biofluid RNA atlas. *Cell Rep.* **33**, 108552 (2020).
- Langevin, S. M. et al. Comparability of the small RNA secretome across human biofluids concomitantly collected from healthy adults. *PLoS ONE* **15**, e0229976 (2020).
- Brown, H. M. Treatment of chronic asthma with prednisolone; significance of eosinophils in the sputum. *Lancet* **272**, 1245–1247 (1958).
- Heaney, L. G. et al. Eosinophilic and noneosinophilic asthma. *Chest* **160**, 814–830 (2021).
- Tosar, J. P. et al. Dimerization confers increased stability to nucleases in 5' halves from glycine and glutamic acid tRNAs. *Nucleic Acids Res.* **46**, 9081–9093 (2018).
- Giraldez, M. D. et al. Phospho-RNA-seq: A modified small RNA-seq method that reveals circulating mRNA and lncRNA fragments as potential biomarkers in human plasma. *EMBO J* <https://doi.org/10.15252/embj.2019101695> (2019).

29. Pliatsika, V. *MINTmap - tRNA fragment (tRF) mapping tool*. Computational Medicine Center at Thomas Jefferson University <https://cm.jefferson.edu/mintmap/> (2020).
30. De Grove, K. C. et al. Dysregulation of type 2 innate lymphoid cells and T2 cells impairs pollutant-induced allergic airway responses. *J. Allergy Clin. Immunol.* **139**, 246–257.e4 (2017).
31. Shigematsu, M., Kawamura, T., Shah, S. D., Deshpande, D. A. & Kirino, Y. RNase 2/EDN cleaves the anticodon loops of tRNAs to produce immunostimulatory tRNA halves in asthma. *bioRxiv* <https://doi.org/10.1101/815803> (2024).
32. Priftis, K. N., Papadimitriou, A., Nicolaidou, P. & Chrousos, G. P. Dysregulation of the stress response in asthmatic children. *Allergy* **64**, 18–31 (2009).
33. Zhang, L., Liu, J. & Hou, Y. Classification, function, and advances in tsRNA in non-neoplastic diseases. *Cell Death Dis.* **14**, 748 (2023).
34. Anderson, P. & Ivanov, P. tRNA fragments in human health and disease. *FEBS Lett.* **588**, 4297–4304 (2014).
35. Zhang, Y. et al. Identification and characterization of an ancient class of small RNAs enriched in serum associating with active infection. *J. Mol. Cell Biol.* **6**, 172–174 (2014).
36. Shen, Y. et al. Transfer RNA-derived fragments and tRNA halves: Biogenesis, biological functions and their roles in diseases. *J. Mol. Med.* **96**, 1167–1176 (2018).
37. Chiou, N. T., Kageyama, R. & Ansel, M. K. Selective export into extracellular vesicles and function of tRNA fragments during T cell activation. *Cell Rep.* **25**, 3356–3370 (2018).
38. Gámbaro, F. et al. Stable tRNA halves can be sorted into extracellular vesicles and delivered to recipient cells in a concentration-dependent manner. *RNA Biol.* **17**, 1168–1182 (2020).
39. Weng, Q. et al. Extracellular vesicles-associated tRNA-derived fragments (tRFs): Biogenesis, biological functions, and their role as potential biomarkers in human diseases. *J. Mol. Med.* **100**, 679–695 (2022).
40. Grosso, J. B. et al. Levels of seminal tRNA-derived fragments from normozoospermic men correlate with the success rate of ART. *Mol. Hum. Reprod.* **27**, gaab017 (2021).
41. Costa, B. et al. Nicked tRNAs are stable reservoirs of tRNA halves in cells and biofluids. *Proc. Natl. Acad. Sci. U. S. A.* **120**, e2216330120 (2023).
42. Yamasaki, S., Ivanov, P., Hu, G.-F. & Anderson, P. Angiogenin cleaves tRNA and promotes stress-induced translational repression. *J. Cell Biol.* **185**, 35–42 (2009).
43. Sultana, M. F., Abo, H. & Kawashima, H. Human and mouse angiogenins: Emerging insights and potential opportunities. *Front. Microbiol.* **13**, 1022945 (2022).
44. Jodar, M. Sperm and seminal plasma RNAs: what roles do they play beyond fertilization?. *Reproduction* **158**, R113–R123 (2019).
45. Liu, S. et al. A tRNA-derived RNA fragment plays an important role in the mechanism of Arsenite -induced cellular responses. *Sci. Rep.* **8**, 16838 (2018).
46. Pawar, K., Shigematsu, M., Sharbati, S. & Kirino, Y. Infection-induced 5'-half molecules of tRNAHisGUG activate Toll-like receptor 7. *PLoS Biol.* **18**, e3000982 (2020).
47. Pawar, K., Kawamura, T. & Kirino, Y. The tRNA half: A strong endogenous toll-like receptor 7 ligand with a 5'-terminal universal sequence signature. *Proc. Natl. Acad. Sci. U. S. A.* **121**, e2319569121 (2024).
48. Pavord, I. D., Pizzichini, M. M., Pizzichini, E. & Hargreave, F. E. The use of induced sputum to investigate airway inflammation. *Thorax* **52**, 498–501 (1997).
49. Spinelli, S. V. et al. miR-30c is specifically repressed in patients with active pulmonary tuberculosis. *Tuberculosis* **105**, 73–79 (2017).
50. Chen, C. et al. Real-time quantification of microRNAs by stem-loop RT-PCR. *Nucleic Acids Res.* **33**, e179–e179 (2005).
51. Max, K. E. A. et al. Human plasma and serum extracellular small RNA reference profiles and their clinical utility. *Proc. Natl. Acad. Sci.* **115**, E5334–E5343 (2018).
52. Krauskopf, J. et al. Application of high-throughput sequencing to circulating microRNAs reveals novel biomarkers for drug-induced liver injury. *Toxicol. Sci.* **143**, 268–276 (2014).
53. Kucsu, C. et al. Integrative analyses of circulating small RNAs and kidney graft transcriptome in transplant glomerulopathy. *Int. J. Mol. Sci.* **22**, 6218 (2021).
54. Wang, X.-J., Gao, J., Wang, Z. & Yu, Q. Identification of a potentially functional microRNA-mRNA regulatory network in lung adenocarcinoma using a bioinformatics analysis. *Front. Cell Dev. Biol.* **9**, 641840 (2021).
55. Yang, P. et al. A novel serum tsRNA for diagnosis and prediction of nephritis in SLE. *Front. Immunol.* **12**, 735105 (2021).
56. Winek, K. et al. Transfer RNA fragments replace microRNA regulators of the cholinergic poststroke immune blockade. *Proc. Natl. Acad. Sci.* **117**, 32606–32616 (2020).
57. Ignacio, C. et al. Alterations in serum microRNA in humans with alcohol use disorders impact cell proliferation and cell death pathways and predict structural and functional changes in brain. *BMC Neurosci.* **5**, 16–55 (2015).
58. Thrash, A., Arick, M. II. & Peterson, D. G. Quack: A quality assurance tool for high throughput sequence data. *Anal. Biochem.* **548**, 38–43 (2018).
59. Langmead, B. & Salzberg, S. L. Fast gapped-read alignment with Bowtie 2. *Nat. Methods* **9**, 357–359 (2012).
60. Chan, P. P. & Lowe, T. M. GtRNAdb 2.0: An expanded database of transfer RNA genes identified in complete and draft genomes. *Nucleic Acids Res.* **44**, D184–D189 (2016).
61. Kalvari, I. et al. Rfam 14: Expanded coverage of metagenomic, viral and microRNA families. *Nucleic Acids Res.* **49**, D192–D200 (2021).
62. Kozomara, A., Birgaoanu, M. & Griffiths-Jones, S. miRBase: From microRNA sequences to function. *Nucleic Acids Res.* **47**, D155–D162 (2019).
63. Kim, D., Paggi, J. M., Park, C., Bennett, C. & Salzberg, S. L. Graph-based genome alignment and genotyping with HISAT2 and HISAT-genotype. *Nat. Biotechnol.* **37**, 907–915 (2019).
64. Quinlan, A. R. & Hall, I. M. BEDTools: A flexible suite of utilities for comparing genomic features. *Bioinformatics* **26**, 841–842 (2010).
65. Schneider, T. D. & Stephens, R. M. Sequence logos: A new way to display consensus sequences. *Nucleic Acids Res.* **18**, 6097–6100 (1990).
66. Magee, R. & Rigoutsos, I. On the expanding roles of tRNA fragments in modulating cell behavior. *Nucleic Acids Res.* **48**, 9433–9448 (2020).
67. Tau, J. et al. Diesel exhaust particles selectively induce both proinflammatory cytokines and mucin production in cornea and conjunctiva human cell lines. *Invest. Ophthalmol. Vis. Sci.* **54**, 4759–4765 (2013).
68. Abramoff, M. D., Magelhaes, P. J. & Ram, S. J. Image processing with ImageJ. *Biophot. Int.* **11**, 36–42 (2004).
69. Tosar, J. P., Castellano, M., Costa, B. & Cayota, A. Small RNA structural biochemistry in a post-sequencing era. *Nat. Protoc.* **19**, 595–602 (2024).

Acknowledgements

The authors would like to thank Dr Uciel Chorostecki (Universitat Internacional de Catalunya) and Dr. Carla Borini (Kresko RNAtch) for their valuable and constructive suggestions during the development of this research work.

Author contributions

C.C. and J.B.G. contributed equally. C.C., J.B.G., L.R.F.A., and S.V.S. conceived the study. L.R.F.A. and M.A. collected the samples. C.C., J.B.G., M.I., M.B.M and S.V.S. performed experiments and analyzed the data. C.C., J.B.G. and S.V.S. discussed and interpreted the results. C.C, J.B.G. and S.V.S. wrote the manuscript. C.C. and J.B.G. prepared the figures and tables. M.I performed bioinformatic analysis. S.V.S., T.M., K.B. and G.B performed experiments in the mouse model and analyzed the data. O.B. and L.R.F.A. reviewed the manuscript. All of the authors read, edited, and approved the final version of the manuscript.

Funding

The article was funded by Agencia Santafesina de Ciencia,Tecnología e Innovación, IO-058-18, Agencia Nacional de Promoción de la Investigación,el Desarrollo Tecnológico y la Innovación, PICT-2021-GRF-TII-00142.

Declarations

Competing interests

The authors declare no competing interests.

Additional information

Supplementary Information The online version contains supplementary material available at <https://doi.org/10.1038/s41598-025-03314-y>.

Correspondence and requests for materials should be addressed to S.V.S.

Reprints and permissions information is available at www.nature.com/reprints.

Publisher's note Springer Nature remains neutral with regard to jurisdictional claims in published maps and institutional affiliations.

Open Access This article is licensed under a Creative Commons Attribution-NonCommercial-NoDerivatives 4.0 International License, which permits any non-commercial use, sharing, distribution and reproduction in any medium or format, as long as you give appropriate credit to the original author(s) and the source, provide a link to the Creative Commons licence, and indicate if you modified the licensed material. You do not have permission under this licence to share adapted material derived from this article or parts of it. The images or other third party material in this article are included in the article's Creative Commons licence, unless indicated otherwise in a credit line to the material. If material is not included in the article's Creative Commons licence and your intended use is not permitted by statutory regulation or exceeds the permitted use, you will need to obtain permission directly from the copyright holder. To view a copy of this licence, visit <http://creativecommons.org/licenses/by-nc-nd/4.0/>.

© The Author(s) 2025